# 2 Heat transfer in critical fluids

This chapter starts with a brief overview of the properties, dynamic and static, of a fluid near its liquid-vapour critical point that are encountered in this thesis. Then, the evolution is considered of the temperature-density field in a compressible fluid, following a plane thermal disturbance into an otherwise homogeneous sample. Gravity-driven phenomena in a critical fluid are discussed in the last section.

## 2.1 The critical state

### 2.1.1 Thermodynamic relations

The thermodynamic behaviour of a fluid is described by means of a relation between parameters defining its state: the pressure $p$, the density $\rho$ (or molar volume $v$) and the temperature $T$. The thermodynamic static or equilibrium properties may be obtained by the mutual derivatives of these and the (molar) entropy $s$. The specific heats at constant pressure $c_p$ and at constant volume $c_v$, which measure the heat absorption from a temperature stimulus, are defined by

$$c_x \equiv T\left(\frac{\partial s}{\partial T}\right)_x \tag{2.1}$$

where $x = p$ or $v$. The isothermal and adiabatic compressibilities, $K_T$ and $K_s$, measure the response to a pressure stimulus. These are defined by the relation

$$K_y \equiv -\frac{1}{v}\left(\frac{\partial v}{\partial p}\right)_y = \frac{1}{\rho}\left(\frac{\partial \rho}{\partial p}\right)_y \tag{2.2}$$

where $y = T$ or $s$. Also there are the coefficients of thermal expansion, $\alpha_p$ and $\alpha_s$, which are defined by

$$\alpha_z \equiv \frac{1}{v}\left(\frac{\partial v}{\partial T}\right)_z = -\frac{1}{\rho}\left(\frac{\partial \rho}{\partial T}\right)_z , \tag{2.3}$$

where $z = p$ or $s$.

It follows from these definitions that these quantities are not independent of one another. Particularly useful relations among them are

$$K_T(c_p - c_v) = \frac{T}{\rho}\alpha_p^2 \tag{2.4}$$

and

$$c_p(K_T - K_s) = \frac{T}{\rho}\alpha_p^2 . \tag{2.5}$$

The specific heat and compressibility are positive for all $T$, hence eqs. (2.4) and (2.5) imply that $c_p \geq c_v$ and $K_T \geq K_s$ †. From eqs. (2.4) and (2.5) it is elementary to obtain that

$$c_p / c_v = K_T / K_s . \tag{2.6}$$

Other familiar relations that will be utilized in this thesis are

$$\alpha_p / \alpha_s = 1 - c_p / c_v \tag{2.7}$$

$$c_v / \alpha_s = -\frac{T}{\rho}\left(\frac{\partial p}{\partial T}\right)_\rho . \tag{2.8}$$

### 2.1.2 Power laws

The generally accepted conjecture is to describe the asymptotic behaviour of the various properties of a fluid near its liquid-vapour critical point (CP), along selected paths in the phase diagram, in terms of simple power laws. With these power laws, critical exponents and power-law amplitudes are introduced. For an exact treatment of this conjecture we refer to e.g. ref. [14].

In the power law description, it is assumed that the properties vary (asymptotically on approaching CP) as a simple power of the distance to CP, expressed either in temperature, density or pressure. With $T_c$, $\rho_c$ and $p_c$ denoting the temperature, density and pressure at the critical point respectively, we introduce $\tau$, the reduced temperature difference, $\tau \equiv (T - T_c)/T_c$, and, analogously, $\phi$, the reduced density difference, $\phi \equiv (\rho - \rho_c)/\rho_c$ and $\psi$, the reduced pressure difference, $\psi \equiv (p - p_c)/p_c$ ‡. One then has, in the limit $\tau \to 0$,

$$p_c K_T = \Gamma \tau^{-\gamma} \tag{2.9}$$

and

† In particular, as $T \to T_c$, $c_p >> c_v$ and $K_T >> K_s$.

‡ Customarily, in literature the symbol $\pi$ is used for the reduced pressure difference . To avoid confusion with the value $\pi$, a different symbol is used.

$$\frac{\rho_c T_c}{p_c} c_v = \frac{A}{\alpha} \tau^{-\alpha} \tag{2.10}$$

where the path is the critical isochore. $\Gamma$ and $A$ are called the critical power-law amplitudes and $\gamma$ and $\alpha$ the critical exponents. Along the critical isotherm, the variation of the pressure with density is given by

$$\psi = D|\phi|^{\delta} sign(\phi), \tag{2.11}$$

and for $\tau < 0$, the asymptotic shape of the coexistence curve is given by

$$|\phi| = B(-\tau)^{\beta}, \tag{2.12}$$

where $D$ and $B$ are the amplitudes and $\delta$ and $\beta$ are the exponents.

From eqs. (2.4)-(2.8) it follows that the divergences of $\alpha_s$ and $K_s$ are equal to that of $c_v$, and that the divergences of $c_p$ and $\alpha_p$ are equal to that of $K_T$.

A relevant length scale in the description of critical behaviour is the correlation length $\xi$ which characterizes the spatial extent of the fluctuations in the local density. This correlation length is believed to be the only length scale needed to describe the properties of a critical system [13], and is represented by

$$\xi = \xi_0 \tau^{-\nu} \tag{2.13}$$

with $\xi_0$ the amplitude and $\nu$ the critical exponent.

A schematic phase diagram of a fluid near its critical point is given in fig. 2.1 in the $\{\rho, T\}$-plane. Indicated are the critical point CP, the critical isochore $(\rho = \rho_c$ for $T > T_c)$ and the curve picturing the coexisting liquid and vapour densities $(T < T_c)$. The power laws are defined asymptotically $(T \to T_c)$ along these paths (except of course eq. (2.11)).

**Figure 2.1** Illustration of the density-temperature phase diagram.

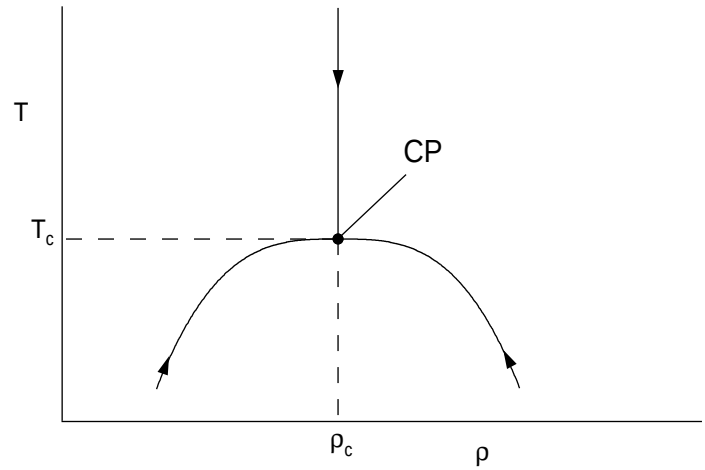


Systems near a critical point are classified in terms of universality classes that depend on the dimensionality of the system and on the number of components of the order parameter. Systems

that belong to the same universality class have the same values for the critical exponents. Pure fluids near their critical point belong to the universality class of three-dimensional Isinglike systems with one order parameter. Thus, the critical exponents are not fluid-dependent and their values are equal to those derived for the Ising systems [14,15,43]. Table 2.1 lists the values for these exponents derived by using the renormalization-group method [15,43,44].

**Table 2.1** Universal critical exponents.

| | | | | |
|---|---|---|---|---|
| $\alpha$=0.11 | $\beta$=0.325 | $\gamma$=1.24 | $\delta$=4.815 | $\nu$=0.63 |

Among the various critical exponents general relations exist. Pure thermodynamics implies

$$\gamma = \beta(\delta - 1) = 2(1 - \beta) - \alpha \tag{2.14}$$

and the principle of universality gives us

$$d\nu = 2 - \alpha \tag{2.15}$$

where $d$ is the dimensionality of the system (for simple fluids: $d = 3$). For a number of amplitudes one also has interesting interrelationships (see e.g. refs. [45-48]).

### 2.1.3 Transport properties

Basic transport parameters are the thermal conductivity $\lambda$, the thermal diffusivity $D_T$ and the viscosity $\eta$. On approaching the critical point, the thermal conductivity is known to diverge. This may be reasoned following a simple, heuristic argument. As usually accepted, we write the heat flux $j$ as a linear function of the temperature gradient. Such an approximation, widely known as Fourier's law, defines phenomenologically the thermal conductivity. Thus, we have [49]

$$j = -\lambda \nabla T . \tag{2.16}$$

One may argue that when the correlation length $\xi$ (see eq. (2.13)) becomes large, the heat flux scales like $j \sim \xi \nabla T$. With eq. (2.16), this implies that, sufficiently close to CP, $\lambda$ behaves roughly as $\xi$. Indeed the critical exponent for $\lambda$ is equal to 0.57 [50], only slightly different from that of $\xi$.

The thermal diffusivity describes the behaviour of a fluid in a non-static temperature distribution and is related to the thermal conductivity through

$$D_T = \frac{\lambda}{\rho c_p} . \tag{2.17}$$

Unlike the thermal conductivity, the thermal diffusivity vanishes on approaching the critical point since the divergence of $\lambda$, although considered strong, is less than that of $c_p$. Near the critical point, $D_T$ should satisfy a Stokes–Einstein relation [51-53]

$$D_T = \frac{R_D k_B T}{6\pi\eta\xi} , \tag{2.18}$$

where $R_D$ is a dimensionless universal amplitude. The viscosity displays a weak divergence [53],

$$\eta \sim (Q_0 \xi)^{\zeta} , \tag{2.19}$$

where $Q_0$ is a system-dependent constant and $\zeta$ is a universal critical exponent equal to 0.063 [50].

## 2.2 Heating a critical fluid

To describe the processes of heat transfer in terms of the transport parameters, we consider the transient heating of a critical fluid confined in a fixed volume $V$, initially at uniform temperature and in equilibrium with its surroundings. The transient heating of the fluid is accomplished by the application of a heat flux $q_f$ into the fluid, at a heater surface $S_h$ deposited on a substrate entirely contained within the fluid. The heat is generated at constant power, starting at time $t = 0$. Since during the heating process heat may be dissipated from the fluid into the various walls of the fluid's container, we will have to consider the effect of this as well. We will study the evolution of the temperature-density field in the fluid over a period of time following the start of the heating.

### 2.2.1 Heat transfer equation and the Piston Effect

In order to find an expression for the temperature field in a locally heated fluid, one might investigate the problem theoretically by seeking solutions of the fully non-linear Navier-Stokes equations, subject to appropriate boundary conditions but in the absence of a gravitational field. This is a very complicated task and, therefore, two somewhat simpler approaches have been adopted in literature. Both of these approaches recognize the existence of two different time scales, namely an acoustic time scale ranging from microseconds to milliseconds and a conduction time scale ranging from seconds to hours or, in fluids very near their CP, even days. In the first simplified approach [24], the unsteady linearized Navier-Stokes equations are solved separately in both regimes. In the second approach [22,23] only time scales much longer than typical acoustic times are regarded and, starting from the general equation of heat transfer which expresses the law of conservation of energy, a heat transfer equation is derived which only has to take into account the thermal conduction and compression-work terms, ignoring fluid flow effects.

The existence of these two time scales is most readily understood by considering the pressure. On the (short) acoustic time scale, local fluctuations, caused by heating, propagate through the fluid as pressure waves; the pressure is neither constant in time nor spatially uniform. On the (longer) conduction time scale, the pressure in the system is essentially spatially uniform though not necessarily constant in time. For the purpose of the experiments described in this thesis, it is sufficient to look only at time scales much longer than typical acoustic times and therefore more convenient to adopt the second approach. The heat transfer equation [54], describing the thermal field in a non-viscous compressible fluid, then reduces to [22,23]

$$\frac{dT}{dt} = \left(1 - \frac{c_v}{c_p}\right)\left(\frac{\partial T}{\partial p}\right)_\rho \frac{dp}{dt} + \frac{1}{\rho c_p}\nabla \cdot (\lambda \nabla T)\,. \tag{2.20}$$

Without the first term on the right hand side eq. (2.20) is the familiar Fourier equation governing heat conduction in incompressible fluids at rest, where temperature changes occur through thermal diffusion at constant pressure. However, in general, in a fluid kept at constant volume the pressure increases with time when heating. The first term on the r.h.s. of eq. (2.20) describes the effect of this. It represents a mechanism known as the 'Adiabatic Effect' (AE) or 'Piston Effect' (PE) [21-24]. Equation (2.20) shows that, for time scales much longer than acoustic times, this pres-

sure term acts uniformly across the entire fluid thereby leaving any existing temperature gradients unaltered.

The importance of the pressure term hinges on the factor $(1 - c_v/c_p)(\partial T/\partial p)_\rho$ which depends on the ratio of the specific heats and on the isochoric thermal pressure coefficient $(\partial p/\partial T)_\rho$, two equilibrium thermodynamic quantities. Typically, in fluids the pressure coefficient varies weakly and the ratio of the specific heats is of order unity. However, for a fluid near its liquid-vapour critical point, whereas $(\partial p/\partial T)_\rho$ behaves smoothly, the ratio of the specific heats $c_v/c_p$ decreases strongly on approaching CP. Consequently, the contribution to the temperature dynamics of a variation of pressure with time in a fluid close to CP may differ significantly from the effect far away from CP. The second term on the r.h.s. of eq. (2.20) (the conduction term) contributes only in the region where temperature gradients are present. This term often is simplified to $D_T \Delta T$ †, disregarding the spatial dependence of $\lambda$. Indeed, numerical simulations show that, with heating pulses typical to the experiments described in this thesis, the resulting temperature and density changes are sufficiently small for the various thermodynamic coefficients of the fluid to be considered constant [29]. The vanishingly small thermal diffusivity of a critical fluid renders the second term on the r.h.s. of eq. (2.20) small; the temperature change due to a gradient slows down dramatically on approaching CP. Physically, the fact that the thermal conductivity diverges means that all heat generated in a heater is transmitted directly into the fluid and not in the heater substrate in accordance to Fourier's law (eq. (2.16)). However, the heat is confined in a very thin layer of fluid close to the heater. Actually, the rapid heating and expansion of the fluid in the boundary layer generates a uniform compression of the bulk of the fluid which causes an isentropic temperature increase throughout the fluid. The first term on the r.h.s. of eq. (2.20) expresses just this isentropic temperature increase:

$$\frac{dT}{dt} = \left(\frac{\partial T}{\partial p}\right)_s \frac{dp}{dt} + D_T \Delta T \,. \tag{2.21}$$

Effectively, the relative contribution of the pressure term to the temperature dynamics increases on approaching CP. Close to the critical point, the different characteristics of the two terms have significant consequences which need to be understood before one attempts to make measurements of any transport parameter.

A one-dimensional representation of the expected temperature profile in the fluid after the onset of heating is visualized in fig. 2.2. The fluid is heated from the left. In this figure, the diffusion layer at the heater side and the additional uniform temperature increase of the bulk fluid $\hat{T}_b(t)$ caused by the PE are indicated. The accent circumflex on quantities refers to the differences from their initial values. It should be realized that, with the instantaneous increase in temperature of the entire fluid, a temperature gradient is created between the fluid and the fluid's container walls, initializing an outward flow of heat through these walls immediately after the onset of heating. At these walls, a diffusion layer will arise also as is shown in this figure. These walls, at which no heat is generated, are referred to as the 'cold' walls.

† The difference being the term $D_T \nabla(\ln\lambda)\nabla T$, which takes into account the spatial dependence of the thermal conductivity. Generally, this term is negligible in comparison to $D_T \Delta T$.

**Figure 2.2** The temperature profile after the onset of heating.

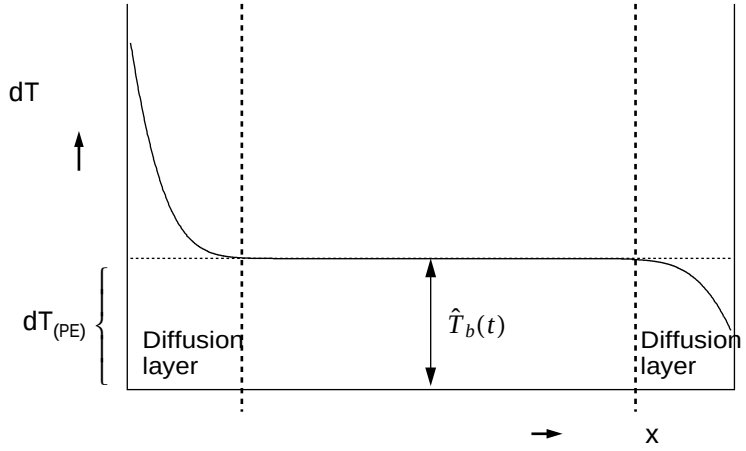


## 2.2.2 Isentropic temperature rise

This section is devoted to the calculation of the temperature rise in the bulk following transient heating, in the approximation that the various thermodynamic coefficients do not vary during heating. In order to find an expression that describes this bulk temperature rise, we will start by considering the temperature rise in the bulk when a quantity of heat $\Delta Q$ is introduced into a small subvolume $V_1$ of the fluid, whose total volume is $V = V_1 + V_2$. If the fluid is free to expand so as to avoid any change in pressure, the temperature and volume of $V_1$ will change by

$$\Delta T_1 = \frac{\Delta Q}{\rho V_1 c_p} \tag{2.22}$$

and

$$\Delta V_1 = \alpha_p V_1 \Delta T_1 , \tag{2.23}$$

respectively. But now, as a second step, the pressure is increased so as to reduce the entire volume by an amount $\Delta V$ back to its original value $V$, thereby cancelling the expansion represented by eq. (2.23). This is accomplished without any entropy exchange, as described by the adiabatic coefficient $\alpha_s$. Substituting $\Delta V = -\Delta V_1$ into the definition for $\alpha_s$, eq. (2.3), and utilizing eqs. (2.7) and (2.22), yields the temperature rise in $V_2$,

$$\Delta T_2 = \frac{-\Delta V_1}{V}\frac{1-(c_p/c_v)}{\alpha_p} = \frac{V_1}{V}\Delta T_1\left(\frac{c_p}{c_v}-1\right) = \frac{\Delta Q}{\rho V c_v}\left(1-\frac{c_v}{c_p}\right). \tag{2.24}$$

The subvolume $V_1$ undergoes the same adiabatic temperature increase. The resulting rise in the average temperature $\langle T \rangle$ for the whole volume is the sum of direct heating on $V_1$ and the adiabatic contribution,

$$\Delta\langle T\rangle = \frac{V_1}{V}\Delta T_1 + \left(\frac{c_p}{c_v}-1\right)\frac{V_1}{V}\Delta T_1 = \frac{\Delta Q}{\rho V c_v}, \tag{2.25}$$

and is determined, as to be expected, by $c_v$, the constant volume specific heat.

Dividing up the process envisioned above into two steps is not essential. The pressure and entropy changes can occur simultaneously so as to keep the total volume unchanged at all times. We may reformulate eq. (2.24) to continuous heating of a critical fluid, so that for a heat flux $q$ the temperature rise outside of the boundary layer in the bulk fluid is:

$$\frac{dT_b}{dt} = \frac{(q - q_l)}{\rho_c V c_v}\left(1 - \frac{c_v}{c_p}\right). \tag{2.26}$$

In eq. (2.26), $q_l$ represents the heat losses to the cell walls in a real experiment. As explained earlier, these losses from the sample must be taken into account, for the diffusion layers at these cell walls (shown in fig. 2.2) act as inverse pistons, or more clearly; isentropic cooling begins simultaneously with the isentropic temperature rise.

Ferrell and Hao [55] studied analytically such a combined heating-cooling process, accounting for the available (for heat exchange) surface area of the container walls and the transport properties of both the fluid and the walls. They present the time dependence of the bulk fluid temperature following the introduction of a pulse of heat $Q$ into the fluid all at one instant $(t = 0)$. Avoiding the long-term behaviour of the fluid, when the developing boundary layers reach the size of the characteristic length of the cell, we reproduce from their work the solution of eq. (2.26) in their specific case:

$$\hat{T}_b(t) = \left(1 - \frac{c_v}{c_p}\right)\frac{Q}{\rho_c V c_v}\exp(t^*)\mathrm{erfc}(\sqrt{t^*}), \tag{2.27}$$

where erfc(=1-erf) is the complimentary error function and

$$t^* \equiv t/t_c. \tag{2.28}$$

The characteristic time $t_c$ for the isentropic equilibration is defined as:

$$t_c \equiv \frac{l_{eff}^2}{D_T}. \tag{2.29}$$

Here

$$l_{eff}^{-1} \equiv \frac{(c_p/c_v) - 1}{V}\sum_{i=1}^{N}\frac{\sigma_i S_i}{1 + \sigma_i} \tag{2.30}$$

represents $(c_p/c_v - 1)/V$ times a weighted sum over the surface areas $S_i$ of the $N$ different wall segments $i$; the weight depends on the inverse thermal impedance ratio $\sigma_i$, defined as

$$\sigma_i \equiv \frac{\lambda_i/\sqrt{D_i}}{\lambda/\sqrt{D_T}}, \tag{2.31}$$

where $\lambda_i$ is the thermal conductivity and $D_i$ the thermal diffusivity of the material of the $i$th wall segment.

Ferrell and Hao [55] analyzed eq. (2.27) and concluded that, as CP is approached $(T \to T_c)$ and the fluid thermal impedance drops below that of the walls, a crossover takes place from a rapid decrease in characteristic time $t_c$, relatively far away from $T_c$, to a weak increase in $t_c$, proportional to the square of the constant volume specific heat.

Complementing the work of Ferrell and Hao [55], for the case that energy is applied to the fluid, not instantaneously but continuously, eq. (2.27) is modified to

$$\hat{T}_b(t) = \frac{1-(c_v/c_p)}{\rho_c V c_v}\int_0^t q(t'^*)\exp(t'^*)\mathrm{erfc}(\sqrt{t'^*})dt', \tag{2.32}$$

where $q(t)$ represents the time dependent energy flux to the fluid. If further, heating pulses of constant flux are utilized to stimulate the fluid then $q(t) = q_f$ and eq. (2.32) becomes accordingly

$$\hat{T}_b(t) = q_f\frac{1-(c_v/c_p)}{\rho_c V c_v}\int_0^t \exp(t'^*)\mathrm{erfc}(\sqrt{t'^*})dt', \tag{2.33}$$

which after some algebra leads to

$$\hat{T}_b(t) = q_f A\left[2\sqrt{\frac{t^*}{\pi}} - 1 + \exp(t^*)\mathrm{erfc}(\sqrt{t^*})\right], \tag{2.34}$$

where

$$A \equiv t_c\frac{1-(c_v/c_p)}{\rho_c V c_v}. \tag{2.35}$$

This $A$ represents an apparent amplitude in eq. (2.34). Obviously, $A$ strongly depends on the distance to CP. Close to CP, where $t_c$ scales proportional to $c_v^2$ (in the region where $\sigma_i<<1$ and $(c_v/c_p)<<1$), it follows from eq. (2.35) that $A$ scales proportional to $c_v$.

Now, it is interesting to look at the critical dependence of the behaviour of the bulk temperature rise following transient heating. Analysing eq. (2.34) reveals two limiting cases. Far from $T_c$, where the thermal impedance of the fluid is much larger than that of the boundaries of the system, i.e. $\sigma_i>>1$, eq. (2.34) reduces to

$$\hat{T}_b(t) = q_f\frac{\sqrt{D_T}}{\lambda}\left(\sum_{i=1}^{N} S_i\right)^{-1}\left[2\sqrt{\frac{t}{\pi}} - \sqrt{t_c}\{1-\exp(t^*)\mathrm{erfc}(\sqrt{t^*})\}\right], \tag{2.36}$$

which indicates that the total surface area of the fluid's container is the most important parameter for the determination of the heat-loss. The prefactor in the temperature increase is then dictated mainly by the ratio $\sqrt{D_T}/\lambda$, the thermal impedance of the fluid. As CP is approached and the thermal impedance of the fluid drops below that of the boundaries of the system, eventually $\sigma_i<<1$, in which case eq. (2.34) yields

$$\hat{T}_b(t) = q_f\left(\sum_{i=1}^{N}\frac{\lambda_i S_i}{\sqrt{D_i}}\right)^{-1}\left[2\sqrt{\frac{t}{\pi}} - \sqrt{t_c}\{1-\exp(t^*)\mathrm{erfc}(\sqrt{t^*})\}\right]. \tag{2.37}$$

As can be seen, for this particular limiting case it is the transport properties of the boundaries that govern the thermal behaviour of the system. At first sight this is somewhat surprising since one would rather expect the temperature rise in the bulk $\hat{T}_b(t)$ to vanish as the isochoric specific heat diverges. A closer look at eq. (2.37) uncovers that the expected slower temperature increase is incorporated in eq. (2.37) into the second term between brackets which counteracts the first term faster and longer for higher values of $t_c$. Interestingly, in either case – far from or close to $T_c$ – for

$t>>t_c$ a simple relation is obtained which predicts an isentropic temperature change proportional to the square root of the heating time.

### 2.2.3 Boundary layers and the Piston Effect

Now that the piston effect has been explored, the attention is directed to the boundary layers and the influence of the PE on these. In appendix A, the differential equation (2.21) is solved for a constant power heat source at the interface of fluid and wall in the approximation that the various thermodynamic coefficients do not vary during heating. Expressions are found for the temperature field near the heater as well as at the 'cold' walls.

Without the PE or at constant pressure the temperature field $\hat{T}_{f,p}(x,t)$ is given by eq. (A.22);

$$\hat{T}_{f,p}(x,t) = \frac{q_f}{S_h\lambda} 2\sqrt{D_T t}\ \mathrm{ierfc}\left(\frac{x}{2\sqrt{D_T t}}\right), \tag{2.38}$$

where ierfc is the integrated complimentary error function. The solution is one-dimensional in the direction perpendicular to the heater surface. The effective diffusion layer thickness, $x_{eff}$, that is implied by eq. (2.38) is

$$x_{eff} = \sqrt{\pi}\int_0^\infty \mathrm{ierfc}\left(\frac{x'}{2\sqrt{D_T t}}\right)dx' = \frac{1}{2}\sqrt{\pi D_T t}\,. \tag{2.39}$$

In this situation, the generated heat is divided between the fluid and the heater substrate by a constant ratio (eq. (A.21)). For a temperature field as described by eq. (2.38) it is possible, in an experiment, to find directly the thermal diffusivity $D_T$ and the thermal conductivity $\lambda$, by fitting eq. (2.38) to $(T,x,t)$-data sets.

However, the inclusion of the PE introduces additional heat flows at all boundaries and, consequently, changes the temperature profile, as indicated in fig. 2.2. At the 'cold' walls these additional heat flows lead to a temperature profile as calculated in appendix A. With

$$x_i^* \equiv x_i/(2\sqrt{D_T t_c})\,, \tag{2.40}$$

the temperature profile in the fluid $\hat{T}_f(x_i,t)$ at the boundary segment $i$ may be written as (eq. (A.14)):

$$\hat{T}_f(x_i,t) = \hat{T}_b(t) - \frac{\sigma_i}{1+\sigma_i} q_f A\, G(x_i^*, t^*)\,, \tag{2.41}$$

where $G(x_i^*, t^*)$ is a function defined by eq. (A.16).

At the heater itself, the PE also affects the boundary layer. The additional temperature rise disturbs the constant ratio at which the generated heat is split up between fluid and substrate and results in a time dependent heat flow into the fluid (see eq. (A.24)). Since the calculations above are based on a constant heat flow into the fluid, this is bothersome. However, as advances from the results in appendix A, the PE and its consequences are completely additive and the heat flow may be separated into a constant heat flow following from the isobaric case (eq. (A.21)) and a time dependent heat flow outwards as a result from the PE. In this view, the heater serves both as a 'heater surface' and as a 'cold' wall and results as obtained earlier are still valid. The temperature

profile, though, is no longer a simple profile like eq. (2.38) but a sum of eqs. (2.38) and (2.41). In fig. 2.3 the expected temperature profile near the heater is displayed as well as the temperature profile in the isobaric case simply added to $\hat{T}_b(t)$. The shaded area in this figure represents the effect of the PE on the shape of the temperature profile.

**Figure 2.3** Temperature profile at the heater.

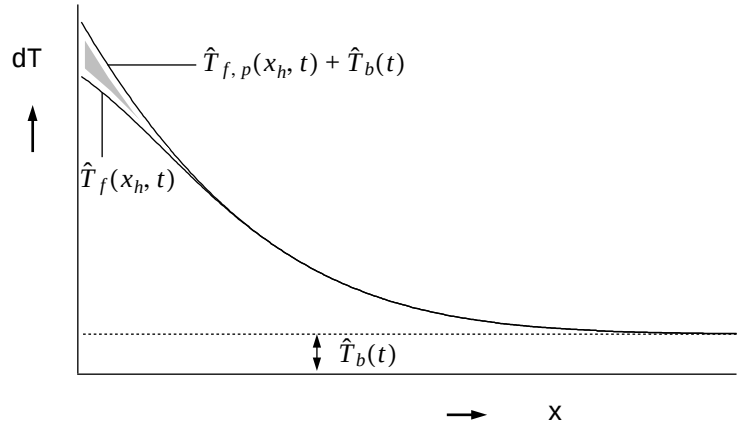


If the transport parameters are to be derived from the resulting temperature profile at the heater, it would be preferable if the position dependent part of this profile, $\hat{T}_f(x_h, t) - \hat{T}_b(t)$, may be considered as equal to the temperature profile $\hat{T}_{f,P}(x, t)$ in the isobaric case; i.e. we would like the shaded area in fig. 2.3 to be insignificant. Some algebra leads to:

$$1 - \frac{\hat{T}_f(x_h, t) - \hat{T}_b(t)}{\hat{T}_{f,p}(x_h, t)} = \frac{\dfrac{\sigma_h S_h}{1+\sigma_h}}{\displaystyle\sum_{i=1}^{N} \frac{\sigma_i S_i}{1+\sigma_i}} \cdot \frac{G(x_h^*, t^*)}{2\sqrt{t^*}\ \mathrm{ierfc}\left(\dfrac{x_h^*}{\sqrt{t^*}}\right)}. \tag{2.42}$$

As shown in appendix B, the second ratio on the r.h.s. of eq. (2.42) is a ratio between two smooth functions, which is always smaller than 1, tends to unity for $x \to 0$ and for $t \to \infty$ and tends to zero for $x \to \infty$ and for $t \to 0$. The interesting part is within the effective size of the boundary layer, $x_{eff}$, where $x^*/\sqrt{t^*} < \sqrt{\pi}/4$ (see eq. (2.39)). In appendix B it is shown that, for $t$ is of the order $t_c$, this ratio is close to 0.5.

When we look at the prefactor on the r.h.s. of eq. (2.42), we again may consider two limiting cases. For $\sigma_i >> 1$, or far from $T_c$, this factor is just the ratio between the surface of the heater $S_h$ and the sum of surfaces of all surrounding walls $S_{tot}$. For $\sigma_i << 1$, or close to $T_c$, the thermal impedances of the walls come into play, making this term a weighted ratio. When $S_h << S_{tot}$ and the thermal impedance of the heater is not much lower than that of the other walls, this factor is much smaller than 1. In appendix B, its value for the actual experimental set up is calculated.

It can be deduced from the aforesaid that we may approach the temperature profile near the heater by a sum of the temperature profile in the isobaric case and the isentropic temperature rise in the bulk when the surface area of the heater is much smaller than the total of the surface area of the surrounding walls or the thermal impedance of the heater is much larger than that of the other

walls. Such an approach would simplify largely the determination of the transport parameters out of the resulting temperature profile.

### 2.2.4 Density changes

In order to find an expression for the changes in the density field, we first write

$$\frac{d\rho}{dt} = \left(\frac{\partial\rho}{\partial T}\right)_p \frac{dT}{dt} + \left(\frac{\partial\rho}{\partial p}\right)_T \frac{dp}{dt}. \tag{2.43}$$

If we substitute $(dp/dt)$ from eq. (2.21) into eq. (2.43), we obtain after some algebra the expression

$$\frac{d\rho}{dt} = -\rho\alpha_s\left\{\frac{dT}{dt} - \frac{c_p}{c_v}D_T\Delta T\right\}. \tag{2.44}$$

It is convenient to introduce the deviation from temperature uniformity

$$\delta T(x,t) \equiv T(x,t) - T_b(t), \tag{2.45}$$

where $T_b(t)$ is the bulk temperature. If we realize that the PE-term in eq. (2.21) is just the time derivative of the isentropic bulk temperature change and that, consequently, the second term on the r.h.s. of eq. (2.21) represents the time derivative of $\delta T(x,t)$, substituting $(dT/dt)$ into eq. (2.44) leads after some algebra to

$$\frac{d\rho}{dt} = -\rho\alpha_s\frac{dT_b}{dt} - \rho\alpha_p D_T\Delta T = -\rho\alpha_s\frac{dT_b}{dt} - \rho\alpha_p\frac{d\delta T}{dt}, \tag{2.46}$$

a relation that enables us to find the density field from the corresponding temperature field.

Equation (2.46) readily demonstrates that the PE alters the density essentially proportional to the temperature, regardless of the distance to the critical point or of the way heat is applied to the fluid. When the fluid is heated, starting from a uniform temperature profile, the second term on the r.h.s. of eq. (2.46) is, in the region outside the developing boundary layer – i.e. in the bulk –, by definition zero. Therefore, provided that the possibly existing density gradients are small enough, simultaneous measurements of temperature and density in the bulk can provide the isentropic thermal expansion coefficient $\alpha_s$.

## 2.3 Bulk temperature induced boundary layers

Earlier, it has been pointed out that, actuated by the PE, at every boundary a diffusion layer will start to develop the moment the fluid is heated. Hence, the temperature-density fields at boundaries at which no heat is generated, i.e. the ‘cold’ walls, are dictated by the evolution of the bulk temperature. In the preceding sections the temperature-density field has been determined for a specific rise of the bulk temperature, namely the one associated with linear heating. In this section, we will consider the developing temperature-density field at the ‘cold’ walls for an arbitrary bulk temperature rise.

### 2.3.1 Temperature lag

An example of the temperature changes at a ‘cold’ wall is displayed in fig. 2.4. Indicated are the bulk temperature change $\hat{T}_b(t)$, the deviation from temperature uniformity in the fluid at the boundary segment $i$ $\delta T(x_i, t)$ and the temperature profile in the wall material $\hat{T}_i(x, t)$.

**Figure 2.4** Temperature change near a ‘cold’ wall.

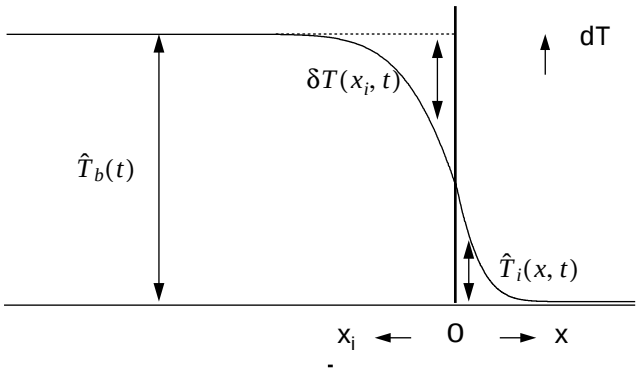


It turns out to be possible to deduce a simple relation between the bulk temperature change and the average temperature change $\langle \hat{T} \rangle$ in a layer of thickness $L$ at a ‘cold’ wall. This average temperature change may be expressed in terms of the bulk temperature change as follows:

$$\langle \hat{T} \rangle = (1 - \Delta_T)\hat{T}_b, \tag{2.47}$$

so that the ‘reduced temperature lag’ $\Delta_T$ is defined as the relative contribution of the temperature changes in the boundary layers to the average temperature change. This definition implies

$$\Delta_T = \frac{1}{\hat{T}_b(t)} \frac{1}{L} \int_0^L -\delta T(x_i, t) dx_i. \tag{2.48}$$

In order to work out further the description of $\Delta_T$, we transcribe the integral part in the Laplace space:

$$\frac{1}{L} \int_0^L \langle \overline{T_b}(s) - \overline{T_f}(x_i, s) \rangle dx_i. \tag{2.49}$$

Substituting from appendix A eq. (A.10) into eq. (2.49) one finds

$$\frac{\sigma_i}{(1+\sigma_i)} \frac{\overline{\hat{T}_b}(s)}{L} \int_0^L e^{-x_i \sqrt{\frac{s}{D_T}}} dx_i = \frac{\sigma_i}{(1+\sigma_i)} \frac{\overline{\hat{T}_b}(s)}{L} \sqrt{\frac{D_T}{s}} \left[ 1 - e^{-L \sqrt{\frac{s}{D_T}}} \right]. \tag{2.50}$$

The inverse Laplace transform of the r.h.s. of eq. (2.50) is [56];

$$\frac{\sigma_i}{(1+\sigma_i)}\frac{2}{L}\sqrt{\frac{D_T}{\pi}}\int_0^t \hat{T}_b(u)\frac{1-e^{-\frac{L^2}{4D_T(t-u)}}}{2\sqrt{(t-u)}}du\,, \tag{2.51}$$

and, with eq. (2.39), eq. (2.48) becomes

$$\Delta_T = \frac{\sigma_i}{(1+\sigma_i)}\frac{2}{L}\sqrt{\frac{D_T t}{\pi}}\int_0^t T_b^*\frac{1-e^{-\frac{\pi(L/x_{eff})^2}{16(1-u/t)}}}{2t\sqrt{(1-u/t)}}du\,, \tag{2.52}$$

where $T_b^* \equiv \hat{T}_b(u)/\hat{T}_b(t)$. Substituting $y \equiv \sqrt{1-u/t}$ and restricting the analysis to the case in which the developing boundary layer is much smaller than $L$ $(x_{eff} << L)$, the integral, $I$, in eq. (2.52) becomes

$$I \equiv \int_0^1 T_b^* dy\,. \tag{2.53}$$

Equation (2.53) shows that $I$ is determined by the history of the bulk temperature change. Hence, in the interpretation in a real experiment, the evaluation of $\Delta_T$ depends on the evolution of the bulk temperature. For a monotone bulk temperature change, it is found easily that $0 < I(t) < 1$ and an upper limit for $\Delta_T$ may be given.

The combination of eqs. (2.52) and (2.53) leads to:

$$\Delta_T(t) = G\sqrt{t}\,, \tag{2.54}$$

where

$$G \equiv \frac{\sigma_i}{(1+\sigma_i)}\frac{2}{L}\sqrt{\frac{D_T}{\pi}}I\,, \tag{2.55}$$

showing that when $I$ is time-independent $\Delta_T$ simply is proportional to $\sqrt{t}$. Equation (2.55) implies a very strong decrease in the factor $G$ as CP is approached since both $\sigma_i$ and $D_T$ vanish on approaching CP. Equation (2.54) can be expressed conveniently in terms of $x_{eff}$ (eq. (2.39)):

$$\Delta_T(t) = \frac{\sigma_i}{(1+\sigma_i)}\frac{4}{\pi}\frac{x_{eff}}{L}I\,. \tag{2.56}$$

Not surprisingly, for $x_{eff} << L$ we find $\Delta_T << 1$.

It follows from eq. (2.53) that $I$ is time-independent if $T_b^*$ can be written as a function of the variable $u/t$. In appendix C it is shown that, in that case, $\hat{T}_b(t)$ must be proportional to $t^{\mu}$ in which case $I$ can be calculated easily as a function of $\mu$. The result is shown in fig. 2.5. It can be shown more generally that for any realistic time dependence of $T_b(t)$ the time dependence of $I$ is of little consequence.

**Figure 2.5** $I$ as a function of $\mu$.

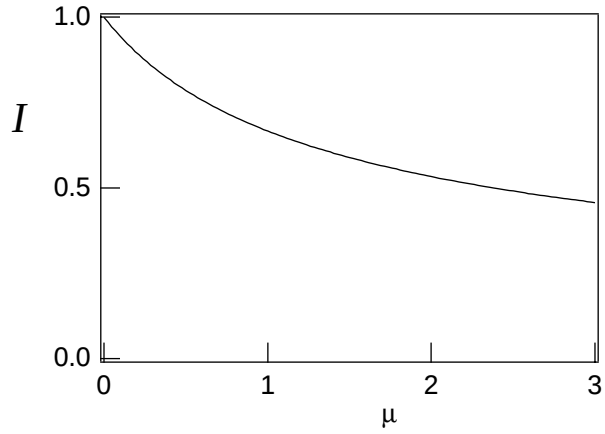


## 2.3.2 Excess density

In order to explore the effect on the density field, we define, in analogy with the deviation from temperature uniformity, the deviation from density uniformity $\delta\rho(x,t) \equiv \rho(x,t) - \rho_b(t)$, where $\rho_b(t)$ is the bulk density. The density profile that correponds to the temperature profile in fig 2.4 is displayed in fig. 2.6, in which $\hat{\rho}_b(t)$ and $\delta\rho(x_i,t)$ are indicated. The density profile in the boundary-layer results from a temperature profile at spatially uniform pressure, therefore:

$$\delta\rho(x,t) = -\rho\alpha_p\delta T(x,t)\,. \tag{2.57}$$

Whereas the temperature changes in the boundary layer are smaller than the bulk temperature change, the density changes in the boundary layer are larger than the bulk density change.

**Figure 2.6** Density change near a 'cold' wall.

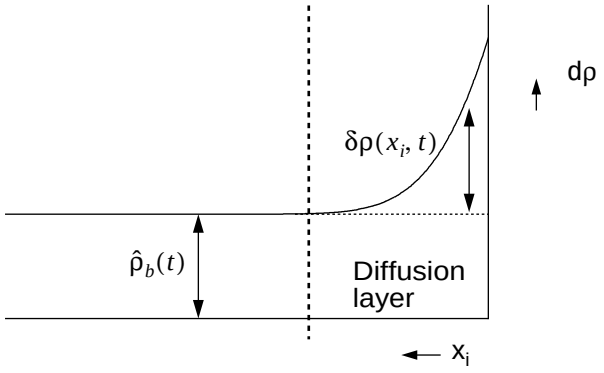


Analogous to $\Delta_T$, we may define a 'reduced excess density' $\Delta_\rho$ by:

$$\langle\hat{\rho}\rangle = (1+\Delta_\rho)\hat{\rho}_b\,, \tag{2.58}$$

where $\langle\hat{\rho}\rangle$ is the average density change. Note the sign in this relation. Equation (2.58) implies

$$\Delta_\rho = \frac{1}{L}\int_0^L \frac{\delta\rho(x,t)}{\hat{\rho}_b(t)}dx, \tag{2.59}$$

so that $\Delta_\rho$ represents the relative contribution of the density changes in the boundary layers to the average density change in a layer of size $L$. In order to relate $\Delta_\rho$ to $\Delta_T$, we first realize that the bulk density change $\hat{\rho}_b$ relates to the bulk temperature change $\hat{T}_b$ as:

$$\hat{\rho}_b(t) = -\rho\alpha_S\hat{T}_b(t). \tag{2.60}$$

Substituting eqs. (2.57) and (2.60) into eq. (2.59) and utilizing eq. (2.7) results in an expression for $\Delta_\rho$ in terms of the temperature profile and finally in terms of $\Delta_T$;

$$\Delta_\rho = \left(\frac{c_p}{c_v}-1\right)\frac{1}{L}\int_0^L \frac{-\delta T(x,t)}{\hat{T}_b t}dx = \left(\frac{c_p}{c_v}-1\right)\Delta_T \equiv E\sqrt{t}, \tag{2.61}$$

where

$$E \equiv \left(\frac{c_p}{c_v}-1\right)G = \left(\frac{c_p}{c_v}-1\right)\frac{\sigma_i}{(1+\sigma_i)}\frac{2}{L}\sqrt{\frac{D_T}{\pi}}I. \tag{2.62}$$

Whereas we could conclude easily that $\Delta_T$ diminishes on the approach to CP, in the case of $\Delta_\rho$ we have to look closer because of the divergence of $c_p/c_v$. Far from CP, where $c_p/c_v$ is of order unity, we may conclude that, for $x_{eff} \ll L$, also $\Delta_\rho \ll 1$. Furthermore, for $\sigma_i \gg 1$, the critical dependence that remains is

$$E \propto \left(\frac{c_p}{c_v}-1\right)\sqrt{D_T}, \tag{2.63}$$

implying an increase in $E$ approaching CP considering the increase of $c_p/c_v$ and the weak decrease of $\sqrt{D_T}$. As CP is approached and the thermal impedance of the fluid drops below that of the boundaries of the system, eventually $\sigma_i \ll 1$, in which case eq. (2.62) yields (with eq. (2.31) and (2.17)) a critical dependence as

$$E \propto \left(\frac{1}{c_v}-\frac{1}{c_p}\right). \tag{2.64}$$

Interestingly, eq. (2.64) shows that, eventually, $E$ decreases on approaching CP as the inverse of the specific heat at constant volume. The actual location of the maximum depends of course on the fluid and the wall material concerned. In fig. 2.7, an example is given for a 8 mm layer of $SF_6$ at a quartz wall, where $I = 0.5$.

**Figure 2.7** The critical dependence of $E$.

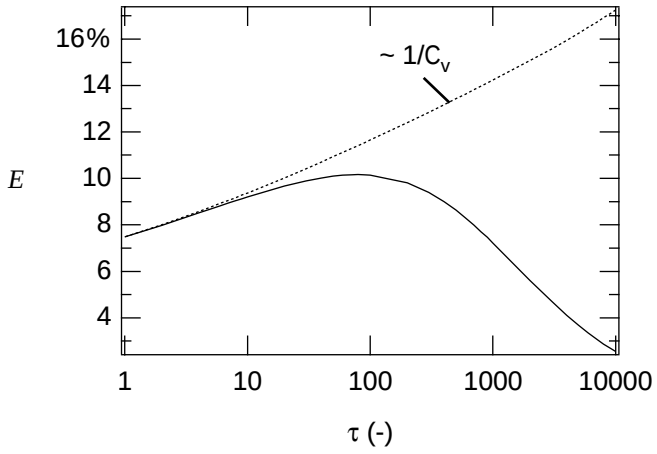


In conclusion, for any realistic bulk temperature rise the relative contribution of the changes in the temperature-density field at a 'cold' wall to the change in average temperature-density field scales like the square-root of the heating time. Such a simple description allows the determination of $\hat{\rho}_b(t)$ by the measurement of $\langle\hat{\rho}(t)\rangle$, which together with the simultaneous measurement of $\hat{T}_b(t)$ can provide $\alpha_s$ as eqs. (2.58) and (2.60) combine to

$$\langle\hat{\rho}(t)\rangle = -\rho\alpha_s(1 + E\sqrt{t})\hat{T}_b(t)\,. \tag{2.65}$$

As long as the effective diffusion layer thickness is much smaller than the layer over which is averaged, the relative contribution of the $\sqrt{t}$-term is small. Moreover, in cases where this contribution is not entirely negligible, knowledge of the time-evolution of $\hat{T}_b(t)$ allows a reasonable estimate for $E$ (see eq. (2.62)). Subsequently, the otherwise difficult to measure value of $c_v$ is determined easily from $\alpha_s$ on account of their interrelationship as expressed by eq. (2.8); the other quantities in this expression are well known and finite, even near CP.

## 2.4 Gravity effects

On earth the behaviour of fluids near their critical point is strongly influenced by gravity. In the gravitational field, the large compressibility of such fluids induces two major effects; a stratification of the fluid forming a density gradient and a strong increase of the susceptibility for convective instability as expressed by the Rayleigh number. In the next sections these gravity-driven phenomena are discussed in order to elucidate the requirement for strongly reduced gravitational levels, such as provided by Spacelab. In the last section it is argued that gravity also may be put to advantage when it is used to monitor the average density of a fluid sample.

### 2.4.1 Density stratification

In the discussion up to this point it has been assumed that the fluid is macroscopically homogeneous. Therefore, the regions over which the integrations are carried out, or through which a beam

of light propagates, were supposed to be characterized by spatially constant values for the thermodynamic values $p$, $\rho$ and $T$. On earth, a critical fluid is subject to a gravitational force and it will be compressed under its own weight. This is compensated for by a gradient in the pressure (the hydrostatic pressure profile) which, in thermal equilibrium, is given by

$$dp = -gM\rho dh, \tag{2.66}$$

where $h$ is the direction of the acceleration of gravity $g$ and $M$ is the molar mass. Using eq. (2.2) it is found that this results in a density gradient given by

$$\left(\frac{d\rho}{dh}\right)_T = gM\rho^2 K_T. \tag{2.67}$$

Due to the divergence of $K_T$ at the critical point, the actual critical conditions are reached only very marginally and local properties may no longer be identified with those of the fluid as a bulk.

In fluids near their critical point, already in small cells density differences are found that, otherwise, are found typically only on an atmospheric scale. To illustrate this, an example of the stratification for $SF_6$ for different temperatures near $T_c$ is shown in fig. 2.8. Each curve is labelled by its temperature difference from $T_c$.

**Figure 2.8** Gravity induced density gradients.

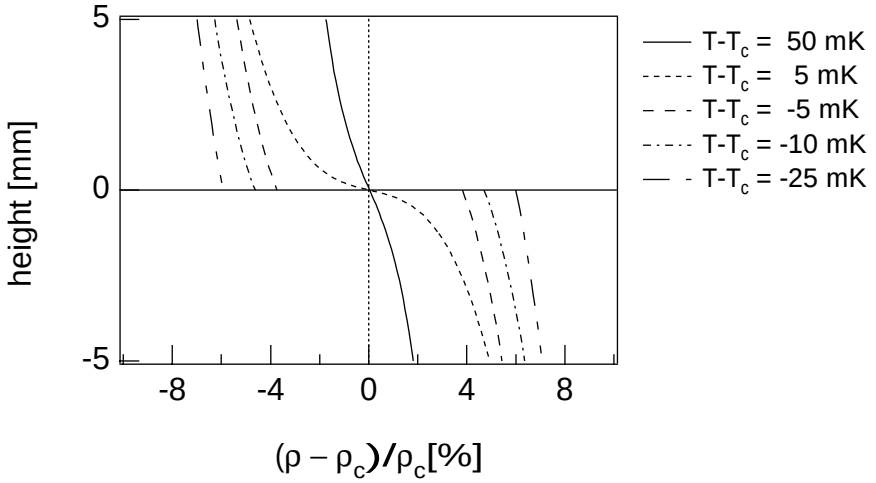


As a consequence of such substantial density gradients, small volumes at different heights within the sample will not be in the same thermodynamic state and the response of the fluid to a plane thermal disturbance will be strongly dependent on height. Also, the transmission and scattering of light will not merely depend on the value of the refractive index but also on its derivative. A ray of light is deviated in an inhomogeneous refractive index field (see Chapter 4).

### 2.4.2 Heating a critical fluid

The response of a critical fluid to a temperature stimulus was calculated in the absence of a gravitational field. In gravity, apart from complications resulting from the density stratification, one has

to consider the susceptibility of a near-critical fluid to convection. Convection instabilities are governed by the Rayleigh number [49]

$$\mathrm{Ra} = \frac{gM\rho\alpha_p h^3 dT}{\eta D_T}, \tag{2.68}$$

where $dT$ is a temperature difference over a height $h$ in the direction of gravity. The high value of the isobaric thermal expansion coefficient leads inevitably to convective motion when temperature disturbances are imposed on the near-critical system.

The phenomenon of convection in compressible fluids has been addressed by several authors [57-61]. Boukari [61] expects from earlier studies that the criterion for the onset of convection changes from the Rayleigh criterion [57] to the Schwarzchild criterion [58] when a critical fluid is brought closer to the critical point. According to this criterion, convection is suppressed when gradients in the direction of gravity are smaller than the adiabatic temperature gradient [59]

$$(\nabla T)_{\mathrm{ad}} = gM\rho\left(\frac{\partial T}{\partial p}\right)_{\rho}\left(1 - \frac{c_v}{c_p}\right). \tag{2.69}$$

Boukari [61] concludes that the adiabatic temperature gradient represents a stabilizing factor against thermal convection for a critical fluid. Although, according to these findings, a critical fluid is more stable than predicted by the Rayleigh criterion, convection remains a serious concern. A quick calculation of $(\nabla T)_{\mathrm{ad}}$ for $SF_6$ shows that its value is close to 1 mK/cm at $\rho_c$ and temperatures within 1 K from $T_c$. The gradients that occur in the experiments described in this thesis often exceed this value.

To a large extent, positive temperature gradients in the direction of gravity may be avoided by conveniently facing the heater downwards. Generally, heating this way the denser parts are found lower into the fluid, in which case convection does not occur. However, due to the PE, gradients will appear on all walls of the fluid's container, including vertical walls at which convection is liable to arise. Since one likes to observe the system parallel to the stratification, i.e. parallel to the heater, in a real experiment these vertical boundaries are impossible to exclude from the field of view. Therefore, whenever convection arises, the field of view most likely will be disturbed by it.

### 2.4.3 The two-phase region

Below the critical temperature, a fluid may be in a state of two coexisting phases with different densities for the vapour $(\rho_v)$ and the liquid $(\rho_l)$ phase. In a gravitational field, the liquid phase is always situated in the lower part of the sample container. The actual position of the meniscus is determined by the difference in density between vapour and liquid (as is determined by the distance to the critical temperature), the average density and the geometry of the sample container. It follows from the classic law of rectilinear diameter that, at temperatures sufficiently close to $T_c$, $\frac{1}{2}(\rho_v + \rho_l) \cong \rho_c$. As a consequence, for an average density equal to the critical density the meniscus will be at the volumetric middle of the container. When the average density is different from the critical density, on approaching the critical temperature, the meniscus will always move away from this middle. This may be clarified as follows: In a container of fixed volume, two processes take place when the sample is heated. The first is that the liquid evaporates; the density of the vapour increases and the volume that the liquid takes up decreases. The second is that the liquid expands; the density of the liquid decreases and the volume it takes up increases (The vapour is more easily compressed and does not expand due to the expansion of the liquid). The effect of the second

increases for higher liquid volumes and, since for an average density equal to the critical the meniscus remains in the middle, we may conclude that the two effects cancel each other out at critical density. For an average density below the critical, the effect of the first dominates while the second dominates for average densities above the critical. Hence, except at critical density, the meniscus will move away from the middle when the temperature is raised towards the critical temperature.

Thus, the position of the meniscus may conveniently be used to determine the average density of the contained sample relative to the critical density. Moreover, the disappearance or reappearance of the meniscus on crossing the critical temperature provides an excellent means to fill the container at critical density, especially when the equation of state of the fluid concerned is not well known.